

**CHARACTERIZATION OF HONEY AS ACTIVE
THIN FILM FOR RESISTIVE SWITCHING
MEMORY APPLICATIONS**

SEAH YING ZHI

UNIVERSITI SAINS MALAYSIA

2022

SCHOOL OF MATERIALS AND MINERAL RESOURCES ENGINEERING
UNIVERSITI SAINS MALAYSIA

**CHARACTERIZATION OF HONEY AS ACTIVE THIN FILM FOR
RESISTIVE SWITCHING MEMORY APPLICATIONS**

By

SEAH YING ZHI

Supervisor: PROF. IR. DR. CHEONG KUAN YEW

Dissertation submitted in partial fulfillment of the requirements for the degree of

Bachelor of Engineering with Honours

(Materials Engineering)

Universiti Sains Malaysia

September 2022

DECLARATION

I hereby declare that I have conducted, completed the research work and written the dissertation entitled 'Characterization of Honey as Active Thin Film for Resistive Switching Memory Applications'. I also declare that it has not been previously submitted for the award of any degree and diploma or other similar title of this for any other examining body or University.

Name of Student: Seah Ying Zhi

Signature:

Date: 09 August 2022



Witness by

Supervisor: Prof. Ir. Dr. Cheong Kuan Yew

Signature:

Date: 09 August 2022



ACKNOWLEDGEMENT

First, I would like to express my thanks and gratitude of Universiti Sains Malaysia and School of Materials and Mineral Resources Engineering for providing me sufficient equipment and workplace to complete this research. I would like to express my sincere gratitude to my supervisor Prof. Ir. Dr. Cheong Kuan Yew for his patience, motivation, invaluable advice, guidance and inspiration throughout the journey of my undergraduate study.

Besides my supervisor, I must extend my deepest appreciation to all technician who have directly and indirectly involved in my research especially Mr. Azam, Mr. Syafiq and Mr. Rashid. I would also like to take this opportunity to thank master and PhD students under Prof Cheong, especially Ms. Lim Ruo Xuan and Mr. Muhammad.

Last but not least, I would like to extend my warmest and heartfelt gratitude to my beloved parents, Seah Chee Beng and Wong Keh Choo who spiritually supports me and giving me encouragement during my hard time with final year projects. Not forgetting, to those who contribute directly or indirectly in this research, thank you so much.

TABLE OF CONTENTS

ACKNOWLEDGEMENT	iii
TABLE OF CONTENTS	iv
LIST OF TABLES	vii
LIST OF FIGURES	viii
LIST OF ABBREVIATIONS	xiii
LIST OF SYMBOLS	xv
ABSTRAK	xvi
ABSTRACT	xviii
CHAPTER 1 INTRODUCTION	1
1.1 Research Background.....	1
1.2 Problem Statement	3
1.3 Objective	4
1.4 Scope of Study	4
CHAPTER 2 LITERATURE REVIEW	6
2.1 Introduction	6
2.2 Resistive Switching Behavior	6
2.3 Evolution of Memory Devices	9
2.3.1 Electrochemical Metallization Mechanism (ECM)	14
2.3.2 Valence Change Mechanism (VCM).....	15
2.3.3 Thermochemical Mechanism (TCM).....	16
2.4 Resistive Switching Materials.....	18
2.4.1 Metal Sulfides Resistive Switching Materials	18
2.4.2 Perovskite Resistive Switching Materials	19
2.4.3 Binary Metal Oxides Resistive Switching Materials	19

2.4.4	Organic Resistive Switching Materials	20
2.4.5	Bio-organic based Resistive Switching Materials.....	21
2.4.6	Polysaccharides Materials	22
2.4.7	Glucose-based Resistive Switching Materials	23
2.4.8	Monosaccharide Fructose-based Resistive Switching Materials ...	24
2.4.9	Honey	25
2.5	Resistive Switching Mechanisms in Bio-organic Thin Film	30
CHAPTER 3 MATERIALS AND METHODOLOGY		35
3.1	Introduction	35
3.2	Raw materials.....	36
3.2.1	ITO glass slide	36
3.2.2	Honey	37
3.2.3	Au-Pd top electrode.....	37
3.3	Experimental Procedure	37
3.3.1	ITO Glass Slide Cleaning.....	37
3.3.2	Honey solution preparation	38
3.3.3	Honey coating	38
3.3.4	Honey thin film fabrication.....	38
3.3.5	Deposition of Au-Pd top electrode.....	39
3.4	Materials Characterization	40
3.4.1	Surface tension and contact angle measurement.....	40
3.4.2	Fourier Transform Infrared Spectroscopy (FTIR) Analysis	40
3.4.3	Differential Scanning Calorimetry (DSC) analysis.....	41
3.4.4	Optical Microscope	41
3.4.5	Scanning Electron Microscopy (SEM)	41
3.4.6	Atomic Force Microscopy (AFM) Imaging.....	41
3.4.7	Semiconductor Parameter Analyzer (SPA).....	42

CHAPTER 4	RESULTS AND DISCUSSIONS	44
4.1	Introduction	44
4.2	Surface tension and contact angle measurement.....	44
4.3	Thermal analysis	47
4.4	Fourier Transform Infrared Spectroscopy (FTIR) Analysis	50
4.4.1	Honey solution with different concentrations	50
4.4.2	Honey coating on ITO glass substrate dried at different temperature.....	57
4.4.3	Honey coating on ITO dried at different duration	62
4.5	Honey coverage observation using optical microscope	66
4.6	Atomic Force Microscopy (AFM) analysis	68
4.7	Semiconductor Parameter Analyzer (SPA).....	74
CHAPTER 5	CONCLUSION.....	83
5.1	Conclusion.....	83
5.2	Recommendation for future work	84
REFERENCES.....		85

LIST OF TABLES

Table 2.1	Summaries of reported polysaccharides-based resistive switching thin film (Modulated from Cheong et al. review paper).	32
Table 3.1	Different drying condition during processing of honey thin film.	39
Table 3.3	Voltage sweeps for I/V measurements.	43
Table 4.1	FTIR peaks of honey solution with different concentrations.	51
Table 4.2	Comparison of FTIR peak area for different honey concentrations. .	55
Table 4.3	FTIR peaks of ITO glass slide and honey coating dried at different temperature.	59
Table 4.4	FTIR peaks of honey coating dried at 100°C for different duration in hours (h).	63

LIST OF FIGURES

Figure 0.1	Schematic of (a) unit cell of resistive switching random access memory and (b) an array of crossbar structure with voltages (V) and current (I) applied and measured, respectively, on top and bottom electrodes (Cheong <i>et al.</i> , 2021).	2
Figure 2.1	(a) Conventional computing architecture (Von Neumann architecture) and (b) Processing-In-Memory (PIM) architecture (Zou <i>et al.</i> , 2021).	7
Figure 2.2	Schematic diagram of a resistive switching device with its application based on their properties (Shi <i>et al.</i> , 2021).	9
Figure 2.3	Classification of memory device.	10
Figure 2.4	(a) Typical current density and voltage plot of a ReRAM device with high-resistance state (HRS) and low resistance state (LRS). Arrows indicates the sweeping directions (Cheong <i>et al.</i> , 2021).....	11
Figure 2.5	Schematic representations of resistive switching in ReRAMs. (a) unipolar resistive switching and (b) bipolar resistive switching (Prakash <i>et al.</i> , 2013).	12
Figure 2.6	Schematic of (a) binary switching behaviour, (b) multilevel switching behaviour, (c) unidirectional analog switching behaviour and (d) bidirectional analog switching behaviour (Zhang <i>et al.</i> , 2019).	13
Figure 2.7	Schematic illustrations on the SET ((a)-(d)) and RESET (e) operations of an ECM cell (Valov <i>et al.</i> , 2011).	14
Figure 2.8	Schematic illustration on the SET and RESET operations of an VCM cell showing a triangular voltage sweep. The green sphere indicates oxygen vacancies while purple sphere indicates Zr ions (Waser, 2012).....	16

Figure 2.9	Thermochemical mechanism of AlO _x based resistive switching device with (a) (b) unipolar switching (c) (d) bipolar switching (Shen <i>et al.</i> , 2020).....	17
Figure 2.10	Various structure of organic resistive switching device (Cho <i>et al.</i> , 2011).	21
Figure 2.11:	Bio-organic resistive switching materials based on polysaccharides....	22
Figure 2.12	Schematic illustration on the resistive switching mechanism in (a) Al/fructose/ITO device and (b) Ag/fructose/ITO device (Xing <i>et al.</i> , 2021).	25
Figure 2.13	Chemical structure of glucose and fructose (a) in cyclic structure and (b) in fischer projection (Charrez, Qiao & Hebbard, 2015).....	26
Figure 2.14	Maillard reaction in honey (Kowalski <i>et al.</i> , 2013).....	28
Figure 2.15	Analog resistive switching behaviour in (a) positive voltage sweep and (b) negative voltage sweep (Sueoka <i>et al.</i> , 2022).	30
Figure 3.1	An overview of experimental process flow	36
Figure 3.2	Honey used along the experiment.....	37
Figure 3.3	Schematic diagram of spin coating process.	38
Figure 3.4	Dried honey thin film on ITO glass slide.....	39
Figure 3.5	(a) Aluminium mask on ITO glass substrate with honey thin film, (b) test structure after Au/Pd top electrode deposition and (c) schematic cross-sectional view of test structure.	39
Figure 3.6	Illustration of test device structure.....	43
Figure 4.1	Surface tension measurement under different honey concentration of (a) 0, (b) 10, (c) 20, (d) 30, (e) 40, (f) 50 weight %.	45
Figure 4.2	Contact angle measurement under different honey concentration of (a) 0, (b) 10, (c) 20, (d) 30, (e) 40, (f) 50 weight %.....	46
Figure 4.3	DSC analysis of honey solution with different concentrations.....	48
Figure 4.4	Chemical structure of 5-hydroxymethyl-2-furfural (5-HMF).....	49
Figure 4.5	FTIR peaks of honey solution with different concentrations.....	50

Figure 4.6	FTIR peaks of different concentration honey solutions with enlargement at specific region (a) single bond region and (b) fingerprint region. Shading area with numbering for area under peak calculation tabulated in Table 4.2.	54
Figure 4.7	Chemical structure of glucose and fructose with hydrogen bonding.	56
Figure 4.8	FTIR peaks of 30% honey coating dried at different temperature for 6 hours.....	57
Figure 4.9	FTIR peaks honey coating dried at different drying temperature with enlargement at specific region (a) single bond region and (b) fingerprint region. Shading area shows indication for area under peak calculation.....	60
Figure 4.10	Comparison of (a) O-H bond and (b) C-O bond in honey thin film dried at different temperature.....	61
Figure 4.11	FTIR stacked peaks of honey coating dried at 100°C for different drying durations.	62
Figure 4.12	FTIR peaks of honey coating dried at different drying durations with enlargement at specific region (a) single bond region and (b) fingerprint region. Shading area with numbering indicates for the peak area calculation.	64
Figure 4.13	Comparison of (a) O-H bond from water and (b) C-H and O-H bond from carbohydrates (c) O-H bond from carbohydrates (d) C-H bond and (e) C-O bond in honey thin film dried at different temperature..	65
Figure 4.14	Optical microscopy images of honey dried at (a)&(e) 100°C (b)&(f) 120°C, (c)&(g) 140°C and (d)&(h) 160°C for 6 hours.....	67
Figure 4.15	Optical microscopy images of honey dried at 100°C for (a)&(d) 9 hours (b)&(e) 12 hours and (c)&(f) 15 hours.	68
Figure 4.16	AFM topographic images for honey dried at (a) 100°C (b) 120°C (c) 140°C and (d) 160°C for 6 hours. The corresponding phase images are shown in (e-h).	70

Figure 4.17	AFM topographic images for honey dried at 100°C for (a) 9 hours, (b) 12 hours and (c) 15 hours. The corresponding phase images are shown in (d-f).....	71
Figure 4.18	SEM images show dried honey film surface with 1.2k magnifications for honey dried at (a) 100°C (b) 120°C (c) 140°C and (d) 160°C for 6 hours. The corresponding AFM tapping mode phase contrast images was shown in (e-h) 2D and (i-l) 3D.	72
Figure 4.19	SEM images show dried honey film surface with 1.2k magnifications for honey dried at 100°C for (a) 9 hours, (b) 12 hours and (c) 15 hours. The corresponding AFM tapping mode phase contrast images was shown in (e-g) 2D and (h-j) 3D.	73
Figure 4.20	Surface roughness obtained from AFM topography images of honey dried at different (a) drying temperature and (b) drying time.....	74
Figure 4.21	I-V hysteresis loop of honey based-RRAM dried at (a) 100°C (b) 120°C (c) 140°C and (d) 160°C for 6 hours. Corresponding semi log I-V plot was shown in (e-h). Arrows showing the direction of voltage sweep while number showing the sequence of voltage sweep.....	77
Figure 4.22	I-V hysteresis loop of honey based-RRAM dried at 100°C for (a) 9 hours, (b) 12 hours and (c) 15 hours. Corresponding semi log I-V plot was shown in (d-f). Arrows showing the direction of voltage sweep while number showing the sequence of voltage sweep.	78
Figure 4.23	Semi log I-V plot of honey-based RRAM dried at (a) different temperature and (b) different duration.	79
Figure 4.24	Summary of I-V characteristic plot showing SET and RESET region.	79
Figure 4.25	Illustration on ON/OFF value obtained for ON/OFF ratio calculation.....	80
Figure 4.26	ON/OFF ratio at different read voltages of honey based-RRAM dried at (a) drying temperature and (b) drying time.....	80

Figure 4.27	Analog plot of honey dried at (a) 100°C (b) 120°C (c) 140°C and (d) 160°C for 6 hours.	81
Figure 4.28	Analog plot of honey dried at 100°C for (a) 9 hours (b) 12 hours, (c) 15 hours.....	82

LIST OF ABBREVIATIONS

5-HMF	5-hydroxymethyl-2-furfural
AFM	Atomic Force Microscopy
BE	Bottom electrode
CNP	Cellulose nanofiber paper
DRAMs	Dynamic random-access memories
DSC	Differential Scanning Calorimetry
ECM	Electrochemical metallization mechanism
EDX	Energy-dispersive x-ray spectroscopy
FRAMs	Ferroelectric random-access memories
FTIR	Fourier Transform Infrared Spectroscopy
GFETs	Graphene field effect transistors
HDD	Hard-disk drives
HRS	High resistive state
IoTs	Internet of Things
ITO	Indium tin oxide
LRS	Low resistive state
MR	Maillard reaction
MRAMs	Magnetic random-access memories
PCM	Phase change memory
PCRAM	Phase change random-access memory
PVA	Polyvinyl alcohol
RAMs	Random-access memories
ReRAMs	Resistive random-access memories

RS	Resistive switching
SAD	Selected area diffractometry
SCLC	Space-charge-limited-conduction
SEM	Scanning Electron Microscopy
SPA	Semiconductor Parameter Analyzer
SRAM	Static random-access memory
STT-RAM	Spin-transfer-torque resistive random-access memories
TE	Top electrode
TCM	Thermochemical mechanism
TEM	Transmission electron microscope
TMV	Tobacco mosaic virus
VCM	Valence change mechanism

LIST OF SYMBOLS

ϵ_r	Dielectric constant
γ_L	Liquid's surface tension
γ_S	Solid's surface energy
R_a	Average surface roughness
R_{rms}	Root mean square surface roughness
$^\circ$	Degree
$^\circ\text{C}$	Degree celsius
wt. %	Weight percentage
ΔH	Enthalpy
mm	Millimetre
nm	Nanometer

CHARACTERIZATION OF HONEY AS ACTIVE THIN FILM FOR RESISTIVE SWITCHING MEMORY APPLICATIONS

ABSTRAK

Peranti pensuisan perintang bio-organik semakin diperhati kerana kesesakan von Neumann dan isu sisa elektronik. Penyelidikan mengenai madu sebagai filem nipis aktif dalam peranti pensuisan perintang bio-organik fokus dalam sifat elektrik. Tujuan penyelidikan ini adalah untuk menyiasat kesan haba terhadap struktur kimia dan komposisi madu dalam mengawal sifat pensuisan rintangan filem nipis madu. Kepekatan madu yang berbeza (0, 10, 20, 30, 40 dan 50 wt.%) dicirikan oleh goniometer, inframerah transformasi fourier spektroskopi (FTIR) dan kalorimetri pengimbangan pembezaan (DSC). Larutan madu 30 wt.% disalut putaran pada slaid kaca ITO 20mm × 20mm dan dikeringkan pada suhu yang berbeza (100, 120, 140, 160°C) dan masa (6, 9, 12, 15 jam). FTIR, mikroskop optik, mikroskopi daya atom (AFM), mikroskop elektron pengimbangan (SEM) dan penganalisis parameter semikonduktor (SPA) digunakan untuk mencirikan filem madu pejal. Dengan mengambil kira keterlarutan madu, 30 wt.% larutan madu dengan sudut sentuhan 44.42° telah dipilih untuk eksperimen seterusnya. Tindak balas endotermik berlaku disebabkan oleh dehidrasi, pencairan, karamelisasi dan tindak balas Maillard dalam campuran madu dan menyebabkan perubahan struktur kimia dalam madu yang ikatan O-H berkurangan. Madu mempunyai liputan yang baik pada slaid kaca ITO dan filem itu agak seragam dan rata kerana purata kekasaran adalah sekitar 0.5424-2.439nm kecuali madu yang dikeringkan pada 100°C selama 6 jam. Peranti ujian Au/Pd/madu/ITO menunjukkan pensuisan analog dengan ciri I-V berbilang peringkat yang memberi manfaat kepada aplikasi sinaps tiruan. Akhir sekali, madu yang dikeringkan pada 100°C selama 12 jam

menunjukkan sifat pensuisan rintangan terbaik disebabkan nisbah ON/OFF yang tinggi pada 1.322 dekat 0.25V.

CHARACTERIZATION OF HONEY AS ACTIVE THIN FILM FOR RESISTIVE SWITCHING MEMORY APPLICATIONS

ABSTRACT

Bio-organic resistive switching (RS) device was gaining more attention due to von Neumann bottleneck and electronic waste issue. Research on honey to be act as active thin film in RS device was mainly on electrical properties. The aim of this research is to investigate the thermal effects towards chemical structure and composition of honey in controlling the resistive switching properties of honey thin film. Different concentration (0, 10, 20, 30, 40 and 50 wt.%) of honey solution was characterized by goniometer, fourier transform infrared spectroscopy (FTIR) and differential scanning calorimetry (DSC). 30 wt.% honey solution was spin coated onto 20mm × 20mm ITO glass slide and dried at different drying temperature (100, 120, 140, 160°C) and time (6, 9, 12, 15 hours). FTIR, optical microscope, atomic force microscopy (AFM), scanning electron microscope (SEM) and semiconductor parameter analyzer (SPA) was used to characterize the solidified honey film. By considering the solubility of honey, 30 wt.% honey solutions with contact angle of 44.42° was chosen for subsequent experiment. Endothermic reactions occur due to dehydration, melting, caramelization and Maillard reaction in honey mixture and causes chemical structural changes in honey which the O-H bond decreases along the heating. The honey has a good coverage on ITO glass slide and the film was relatively uniform and flat as the average roughness was around 0.5424-2.439nm except for honey dried at 100°C for 6h. The Au/Pd/honey/ITO test device shows analogous switching with multilevel I-V characteristic that benefits artificial synapse applications. Lastly, honey dried at 100°C for 12h shows the best resistive switching properties due to high ON/OFF ratio of 1.322 at 0.25V.

CHAPTER 1

INTRODUCTION

1.1 Research Background

Electronic waste has been a global issue due to the fast development of technologies and shorter useful lifespan of electronics. The waste electrical and electronic equipment (WEE) forum reported that an estimated 57.4 million tonnes of electronic waste was generated in year 2021 (WEEE Forum, 2021). Owing to the expansion of technologies, affinity towards purchase of multiple and newest electronic devices such as smartphone, tablets, laptops etc. are inevitable in this era, thus the generation of associated waste are unavoidable. Older electronic gadgets were disregarded or disposed before reaching its operational lifecycle limit as it tends to be replaced by more advanced function devices (Nithya *et al.*, 2021). The disposal of electronic devices often come together with the memory components. The architecture of the memory components was based on traditional von Neumann architecture initially but now it has reached its limitation. The increase in big data due to Internet of Things (IoTs) driven by Industrial Revolution 4.0 (IR 4.0) causes high demand on cost-effective, simpler manufacturing process and higher memory density device. Thus, resistive switching memory device are gaining more attention (Wang *et al.*, 2020).

Resistive switching materials that enable to provide high throughput, energy-efficient, multistate programmability, good endurance and high speed were chosen for memory storage application. Resistive switching memory device able to store the information in the form of electrical bias depends on their resistance states (Wang *et al.*, 2020). Normally, the resistive switching devices are in the form of a metal-

dielectric-metal two-terminal junction constructed in a crossbar architecture as shown in Figure 1.1 (Cheong *et al.*, 2021).

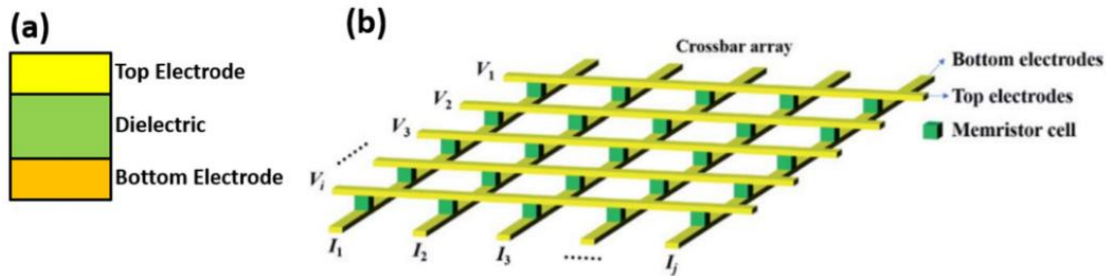


Figure 0.1 Schematic of (a) unit cell of resistive switching random access memory and (b) an array of crossbar structure with voltages (V) and current (I) applied and measured, respectively, on top and bottom electrodes (Cheong *et al.*, 2021).

In selecting and developing materials for electronic memory application, material's sustainability has become one of the major concerns. Therefore, the potential of using bio-organic materials for electronic applications has been aggressively researched to address the issue of material sustainability (Cheong *et al.*, 2021). There were extensive reports on the use of inorganic, polymer and natural bio-organic materials as active thin film for resistive switching memory applications. As reviewed by Wang *et al.*, the resistive switching properties of inorganic-oxide-based thin film was governed by either electrochemical reactions, phase changes, tunnel magnetoresistance or ferroelectricity. Although inorganic based thin film shows excellent contribution towards non-volatile memory application due to its high reliability, low operating power, high operating speed and small footprints, it faces the issue on materials and environmental sustainability. Thus, bio-organic based active thin film was introduced to overcome this issue as it biodegradable, sustainable and environmentally friendly. Although the performances of bio-organic-based resistive switching memory device are not as good as inorganic-based memory device, the bio-organic-based memory device could be used in electronic device that required short

operating lifetime as the technology is emerging and been replaced by newer function rapidly (Cheong *et al.*, 2021).

In this project, a natural existing bio-organic materials that contains polysaccharides which is honey were used as an active thin film for the resistive switching memory application. The reported research on the possibilities of honey to be utilize as active thin film in resistive switching application was mainly based on its electrical properties (Sivkov *et al.*, 2020). However, there is no studies on the physical, chemical and optical properties of the honey thin film. Thus, this project was focus on how the chemical composition and structure in the processed honey in different concentration, drying temperature and time affects its resistive switching properties.

1.2 Problem Statement

Bio-organic materials derived from living or once-living organisms have emerged as an alternative to semiconductor or synthetic polymer for low cost and renewable resistive switching memory device with benefits of environmentally benign, bioresorbable, bio-compatible and biodegradable as compared to inorganic and polymeric materials. Moreover, it is also able to address with two global challenges by today's computing systems which are tremendous energy consumption and electronic waste. Honey was chosen among the natural materials as it is widely available and does not require extensive processing. Honey thin film was reported to exhibits resistive switching properties based on the polysaccharide, main components in honey. Honey contains mostly glucose and fructose which is the sugar molecules, thus it is in the categories of polysaccharides resistive switching bio-organic materials. However, the ability of honey to act as promising active thin film in resistive switching memory application mainly depends on charge conducting mechanism in honey active thin film.

Although extensive studies involving honey thin film in resistive switching application, relatively little effort has been put into investigating the chemical, optical and thermal properties of honey thin film. More work is necessary to investigate the attribution of chemical structure in honey in governing the resistive switching state. The question now is how the chemical and physical properties of honey can be used to explain the charge conduction mechanism during the resistive switching states. Thus, the characterization on honey would be useful to give a deeper look on how the chemical structure affects the resistive switching properties of honey. A honey active thin film sandwiched between Au-Pd as top electrode and ITO-coated glass substrate will be investigated for its resistive switching properties in this project. The importance of our work lies in the fact that thermochemical characteristic of honey can be extended to resistive switching properties.

1.3 Objective

The objectives of this project are:

1. To determine the concentration of honey in affecting the wettability of honey mixture on ITO glass substrate.
2. To investigate the effects of drying temperature and time during processing of honey thin film on the switching behaviour of honey thin film.

1.4 Scope of Study

This dissertation consists of five chapters. The first chapter starts with introduction which the research background, problem statement and scopes of study are being discussed. Next, Chapter 2 is the literature review for the research project.

Chapter 2 will mainly discuss about resistive switching behaviours, followed by the evolution of memory device and general mechanism of resistive switching device. Besides that, Chapter 2 also discussed the motivation to investigate the honey as bio-organic active thin film for resistive switching applications. The following Chapter 3 will discuss the raw materials, experimental procedures and characterization techniques used throughout the research project to investigate the honey thin film as resistive switching layer. Then, Chapter 4 includes the results analysis and discussion on this project. Finally, Chapter 5 will conclude the entire outcome of the research project. Recommendations for future works are also being suggested in this final chapter.

CHAPTER 2

LITERATURE REVIEW

2.1 Introduction

This chapter reviews the key literature concerned with bio-organic material to be used as an active thin film in a resistive switching memory device. Given that the possibilities of honey to act as a switching layer in a resistive switching memory device have been proven by scholars. However, those studies are predominantly focused on their electrical properties and lack of analysis on the physical, optical and thermal properties of honey thin film. The resistive switching behaviour of honey thin film may be affected by the chemical structure and bonding in the honey thin film. Thus, this review critically evaluates the data in the available literature in a bid to address this gap. This chapter begins with the explanation on resistive switching behaviour which includes the resistive switching device, categories of memory device and general mechanism in resistive switching. Then, the materials used for resistive switching device will be briefly explained based on inorganic and organic broad categories. Bio-organic based resistive switching materials will be our main topic and will be critically review on the reported natural materials used and their resistive switching mechanism. Finally, honey as resistive switching thin film will be discussed extensively.

2.2 Resistive Switching Behavior

Resistive switching behaviour is a characteristic of a material that possess tunable resistance states when induced by an external electrical bias (Wang *et al.*, 2020) while a resistive switching device is a device that could include memory and computation functions in a single cell (Shi *et al.*, 2021). The traditional digital computer

was based on Von Neumann architecture in past decades. However, continuous development on data-centric computing causes frequent data shuttling in Von Neumann architecture not an ideal way when considering their energy efficiency and data bandwidth. In order to solve with the traditional von Neumann architecture bottleneck where the memory and computation units were physically separated, it was shown that by changing the architecture into a concept which information is processed at the site where it is stored could solve this computer-centric architecture problem (Shi *et al.*, 2021). Figure 2.1 below shows the differences between traditional Von Neumann architecture and Processing-In-Memory (PIM) architecture.

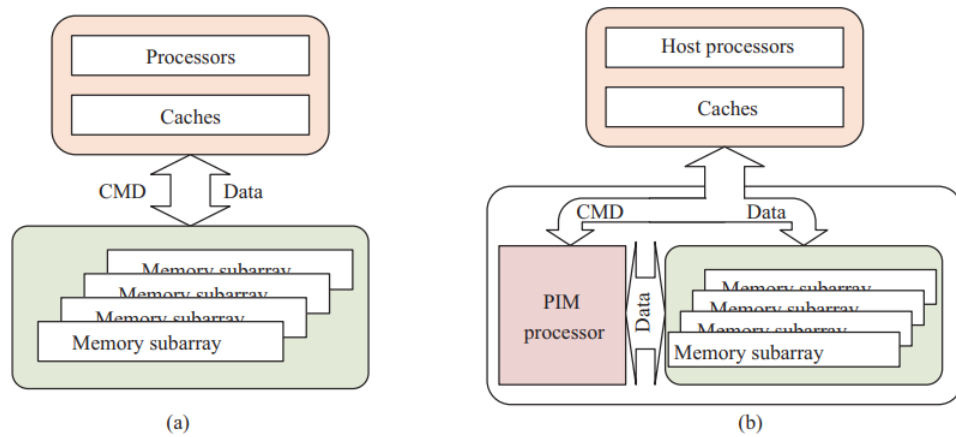


Figure 2.1 (a) Conventional computing architecture (Von Neumann architecture) and (b) Processing-In-Memory (PIM) architecture (Zou *et al.*, 2021).

In PIM system, both the host processor and PIM processor will handle the data which data processing could be done at place which it was stored (Zou *et al.*, 2021). To enable data to be processed at the place where it is stored, a resistive switching material is needed as it could store information in the form of electrical resistance depends on their electrical bias history (Wang *et al.*, 2020).

Research on resistive switching device was started since 1960s where Hickmott (1962) reported negative differential resistance in Al-SiO-Au, Al-Al₂O₃-Au, Ta-Ta₂O₅-

Au, Zr-ZrO₂-Au and Ti-TiO₂-Au system by anodizing the metal in suitable electrolyte. Although the mechanism responsible for negative resistance was uncertain at that time but space-charge-limited currents in the insulators would be the possible mechanism governing the current-voltage curves as stated by Hickmott (1962). In 1971, Chua proposed the analytic theory of memristor as the fourth circuit element. Memristor has the characteristic of which it can remember the currents or charges that previously passed through it (Chua, 1971). Since then, the connections between resistive switching and memristors was established by Yang *et al.* (2008) from Hewlett-Packard (HP) Laboratories in their studies of TiO₂ junction with Pt electrodes which shows fast bipolar non-volatile switching. Research of Yang *et al.* (2008) showed experimental evidence of memristor concept in explaining the switching characteristics of TiO₂ layer. The resistive switching of Pt/TiO₂/Pt was bipolar, reversible and non-volatile with ON/OFF ratios of $\sim 1 \times 10^3$ which was due to the localized oxygen vacancy drifting in the Pt/TiO₂ interface.

Since then, resistive switching device started to become a hot research topic. It was widely accepted that resistive switching device not only provide capabilities for non-volatile data storage but also could be used in data processing and security device due to its unique properties such as high switching speed, high density and low power consumption (Wang *et al.*, 2020; Shi *et al.*, 2021). Figure 2.2 shows various applications of resistive switching device based on their current-voltage characteristics. Analog resistive switching can be used for mimicking synaptic plasticity in neuromorphic computing while digital resistive switching is suitable for memory applications (Shi *et al.*, 2021). To add on, resistive switching that possess cycle-to-cycle variation properties is suitable for data security which has physical unclonable functions (PUFs). The cycle-

to-cycle variation works by giving different resistance than the previous time depending on the previous current that passed through the device (Ibrahim *et al.*, 2022).

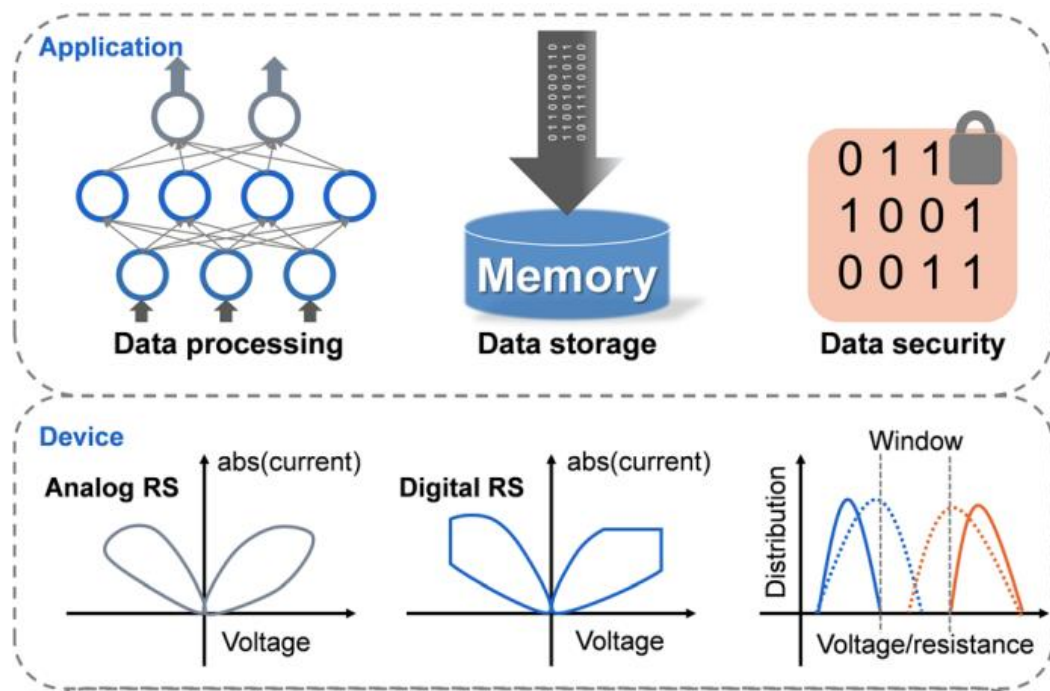


Figure 2.2 Schematic diagram of a resistive switching device with its application based on their properties (Shi *et al.*, 2021).

2.3 Evolution of Memory Devices

Memory device can be classified into volatile (VM) and non-volatile memories (NVM) as shown in Figure 2.3. Volatile memories require constant power to remember the state while non-volatile memories are capable to remember the data without power. So far, the existing memory used for temporary and permanent data storage were VM-type dynamic random-access memory (DRAM) and static random-access memory (SRAM) and NVM-type flash memory (Ibrahim *et al.*, 2022). Although those memories were widely used due to their own advantages, there are still having limitations that difficult to overcome. In general, SRAM is the fastest in “write” and “erase” speed of 100ps but it takes up a lot space on wafer (Ibrahim *et al.*, 2022). DRAMs have a higher switching speed and larger number of write-erase cycles, but they are volatile and need

to refresh frequently. Additionally, flash memories suffer with high power, low write-erase speeds of 0.1-1ms, low number of rewrite cycles about 10^6 and poor endurance as compared to DRAMs (Ouyang, 2016). Thus, a highly non-volatile, scalable memory device with low power, ultra-fast and high endurance and retention capacities are needed for next-generation technologies.

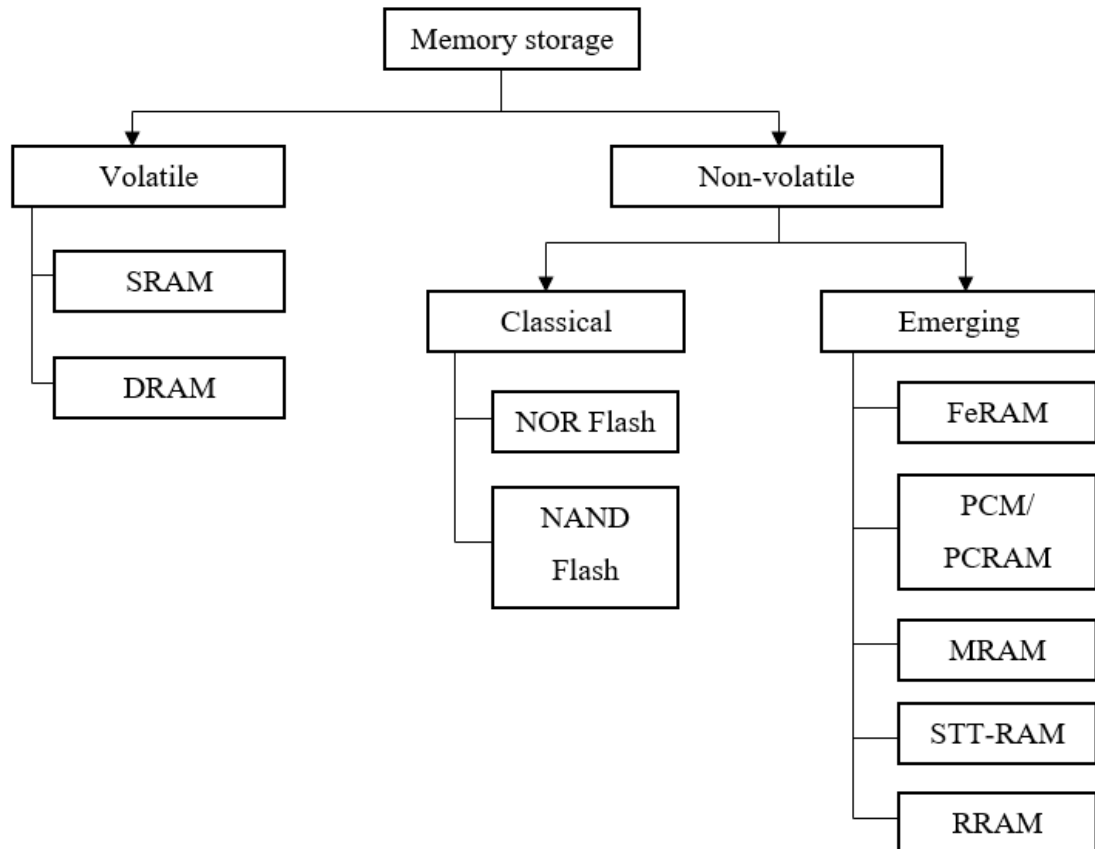


Figure 2.3 Classification of memory device.

As shown in Figure 2.3, the classical non-volatile memories are NOR and NAND flash memories. The differences between these two types of flash memories are their logic configurations. Typically, NOR flash memory was used to store computing instructions or programming code as it has a faster “read” over “write” operation while NAND flash memory was used for mass data storage (Bez *et al.*, 2003). In the emerging categories of non-volatile memory consists of ferroelectric random-access memory

(FeRAM), phase change memory (PCM), magnetic RAM (MRAM) and spin-transfer-torque RAM (STTRAM). Among them, ReRAMs has been continuously explored due to its size miniaturization which the size can be in nanoscale and their response time can be in nanoseconds (Slesazek and Mikolajick, 2019).

Resistive switching memories also named as memristor or ReRAMs that poses tunable resistance states. When a voltage is applied to the devices, they can be switched to a high resistance state (“ON” states) and low resistance state (“OFF” states). The switching from OFF states to ON states is the “set” or “write” process while in reverse switching is it a “reset” or “erase” process. The typical current-voltage plot of a ReRAM device was shown in Figure 2.4(a). A memristive device is composed of an active layer sandwiched between two metal electrodes in a form of metal/insulator/metal (MIM) structure (Figure 2.4) (Ouyang, 2016). The switching layer is the key layer that govern the device performance and will be discussed later.

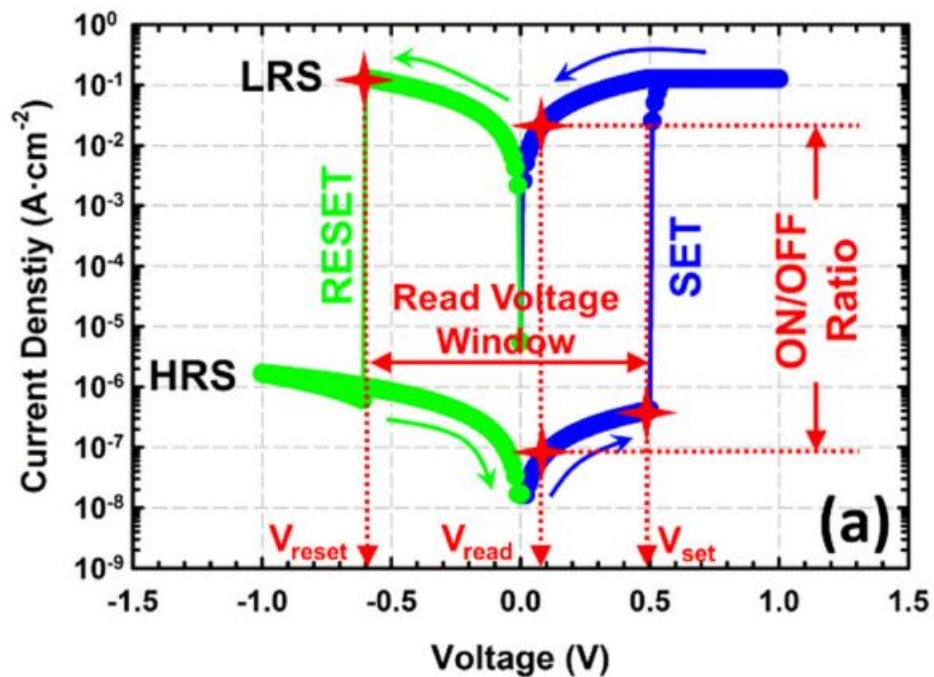


Figure 2.4 (a) Typical current density and voltage plot of a ReRAM device with high-resistance state (HRS) and low resistance state (LRS). Arrows indicates the sweeping directions (Cheong *et al.*, 2021).

Resistive switching in the device can be classified based on current-voltage curves which are unipolar and bipolar switches as shown in Figure 2.5 below. For unipolar switching in Figure 2.5 (a), the switching direction does not depend on polarity of applied voltage which the SET and RESET process are normally in same polarity. However, for bipolar switching in Figure 2.5 (b), the SET and RESET process happens in opposite polarity (Prakash *et al.*, 2013). Additional categories of resistive switching behaviour were stated by Zhang *et al.* (2019) which are multilevel switching behaviour (Figure 2.6(b)), unidirectional analog switching behaviour (Figure 2.6(c)) and bidirectional analog switching behaviour (Figure 2.6 (d)). The binary switching behaviour in Figure 2.6 (a) is the same as bipolar switching in Figure 2.5 (b), just that the presentation in Figure 2.6 (a) is in semi log current-voltage scale.

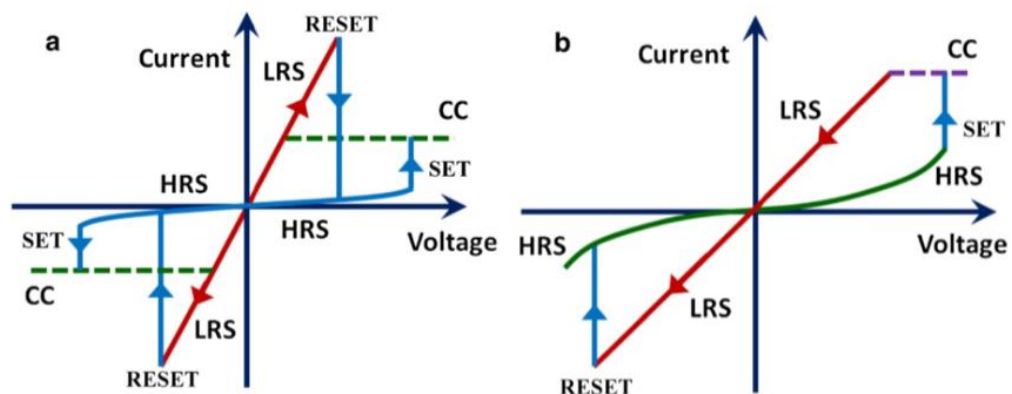


Figure 2.5 Schematic representations of resistive switching in ReRAMs. (a) unipolar resistive switching and (b) bipolar resistive switching (Prakash *et al.*, 2013).

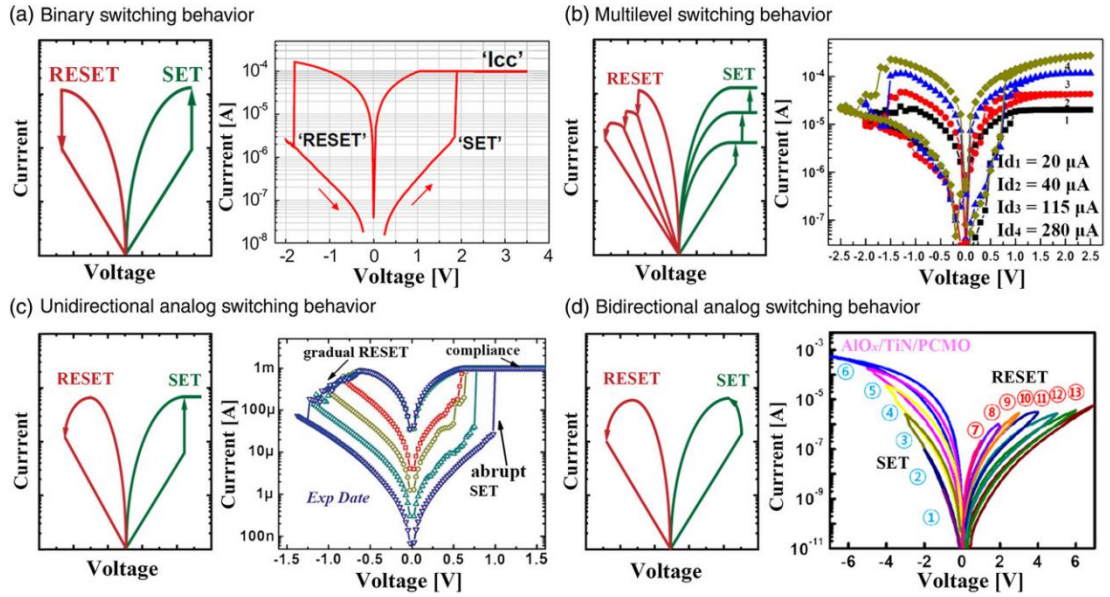


Figure 2.6 Schematic of (a) binary switching behaviour, (b) multilevel switching behaviour, (c) unidirectional analog switching behaviour and (d) bidirectional analog switching behaviour (Zhang *et al.*, 2019).

As reviewed by Zhang *et al.* (2019), binary switching consists of two stable states with abrupt SET and RESET while multilevel switching consists of multiple states which could be controlled by modulating the SET compliance current or RESET voltage. Both binary and multilevel switching behaviour favours data storage applications while unidirectional and bidirectional analog switching behaviour favours neuromorphic applications. For unidirectional analog switching, either SET or RESET was gradual but bidirectional analog switching has both gradual SET and gradual RESET. Thus, the bidirectional analog switching could be used for building neural networks with adaptive learning capability while unidirectional with gradual RESET only is favourable for adaptive learning (Zhang *et al.*, 2019).

Other than that, resistive switching behaviour could also be classified according to their mechanism. As such, the mechanism governing the resistive switching behaviour can be roughly categorized into electrochemical metallization mechanism (ECM), valence change mechanism (VCM), thermochemical mechanism (TCM) and pure electrical/electrostatic effect mechanism (Shi *et al.*, 2021).

2.3.1 Electrochemical Metallization Mechanism (ECM)

Electrochemical metallization mechanism (ECM) happens when a solid electrolyte sandwiched between an electrochemically active electrode such as Ag, Ni, Cu, etc. and an inert electrode such as Pt, Pd, Au, TiN, W, etc. The mechanism was basically due to the redox reactions that forms a conductive filament inside the resistive switching layer. The formation or rupture of conductive filaments corresponds to the transitions of low resistive state (LRS) and high resistive state (HRS) (Shi *et al.*, 2021). Figure 2.7 below shows the schematic illustration of SET and RESET process of an ECM cell.

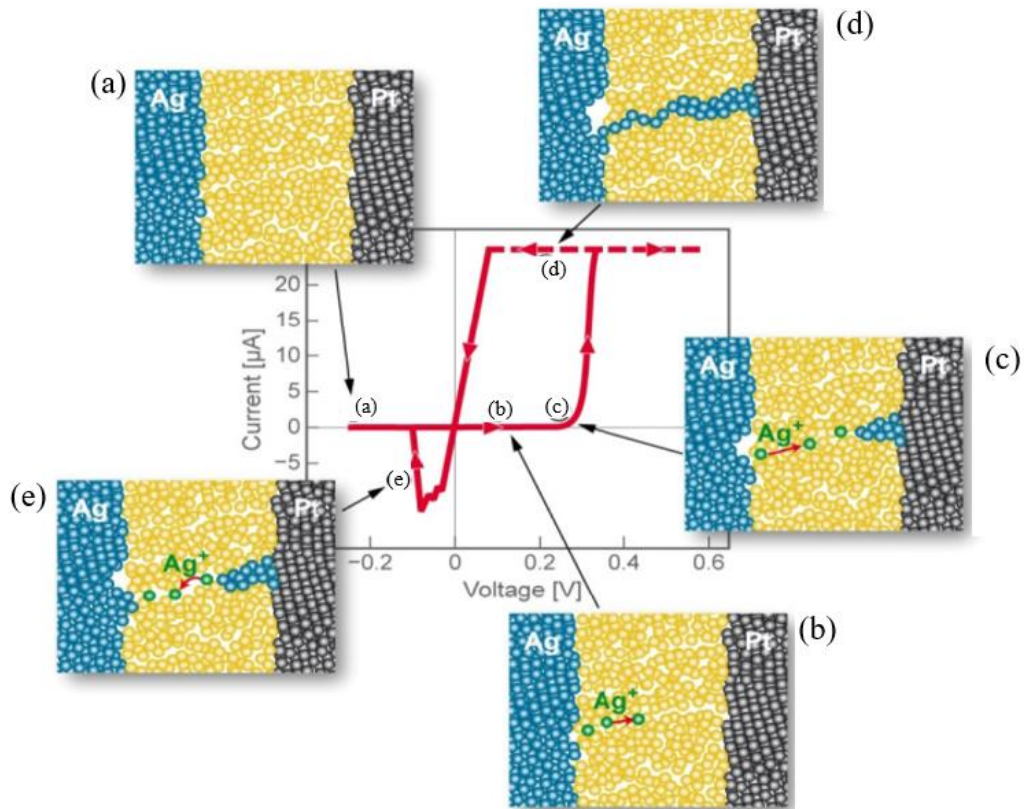


Figure 2.7 Schematic illustrations on the SET ((a)-(d)) and RESET (e) operations of an ECM cell (Valov *et al.*, 2011).

Initially (Figure 2.7(a)), there is no electrodeposition in the electrode which the cell is in a high resistance state (HRS or OFF states). SET process occurs when positive

bias voltage is applied to the Ag electrode. Anodic dissolution of Ag occurs and the Ag^+ cations drift across the electrolyte under electric field formed (Figure 2.7(b)). Cathodic deposition reaction causes the Ag^+ cations reduced to Ag and accumulate on the surface of inert Pt electrode (Figure 2.7(c)). The high electric field leads to formation of conductive filament grow towards the active electrode and when the filament successfully contacts the Ag active electrode, the cell is switched to low resistance state or ON state (Figure 2.7(d)). The ON state will remain unless a negative bias is applied and the Ag conductive path will rupture as the metal dissolution occurs and RESETs the cell (Valov *et al.*, 2011).

2.3.2 Valence Change Mechanism (VCM)

In valence change mechanism (VCM), oxygen vacancies play an important role. VCM is different from ECM which the conductive filaments were form by the oxygen vacancies exchange reactions inside the resistive switching layer. VCM could also happens at the interface of resistive switching layer and originates from the modulation of Schottky barrier at the interface. The difference between metal work function and electron affinity control the resistive switching process (Shi *et al.*, 2021). Figure 2.8 shows the schematic illustration of SET and RESET process of an VCM cell.

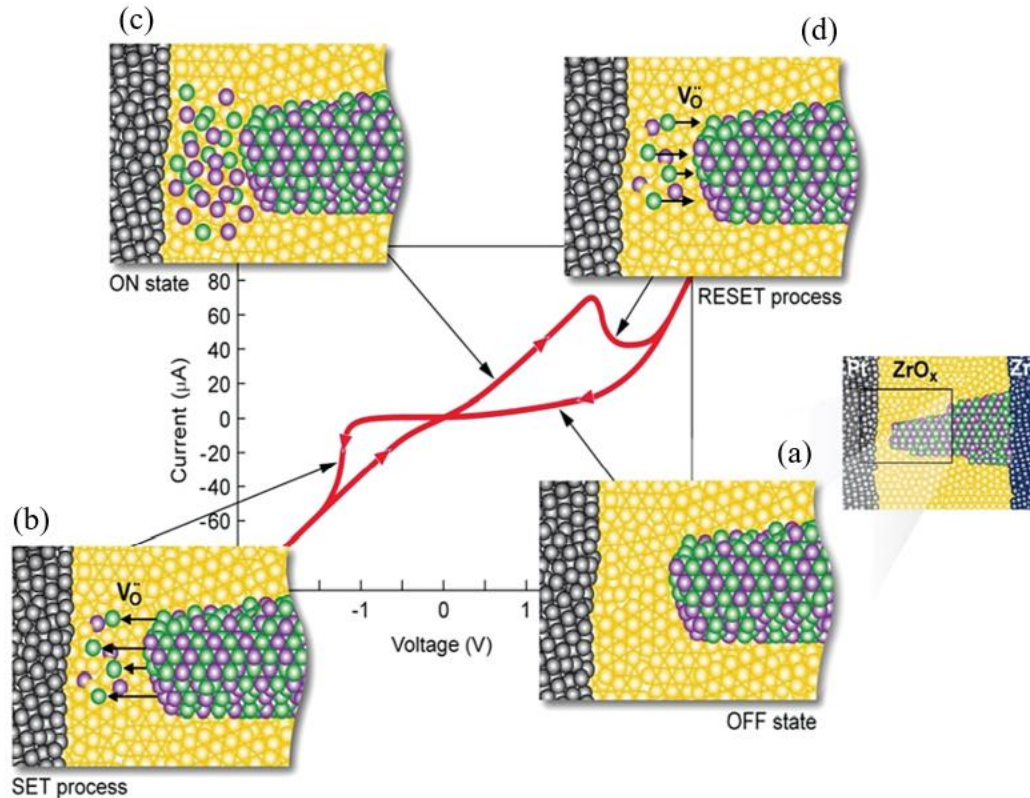


Figure 2.8 Schematic illustration on the SET and RESET operations of an VCM cell showing a triangular voltage sweep. The green sphere indicates oxygen vacancies while purple sphere indicates Zr ions (Waser, 2012).

Initially, the VCM cell is in OFF state which consist of a filament with oxygen vacancies accumulated near the Zr electrode (Figure 2.8(a)). When a negative bias voltage is applied, oxygen vacancies are attracted towards the Pt electrode (Figure 2.8(b)) and switches the device to ON state (Figure 2.8(c)). For the RESET process, when positive bias voltage is applied, Pt electrode repels the oxygen vacancies leads to local re-oxidations and turns the cell into OFF state (Figure 2.8(d)) (Waser, 2012). In VCM, the reaction is anion-based while for ECM, the reaction is cation-based (Kim, Kim & Jang, 2021).

2.3.3 Thermochemical Mechanism (TCM)

Thermochemical mechanism (TCM) usually happens due to thermal effect which influence the unipolar and bipolar resistive switching process. Joule heating

effect was believed to induce the rupture of conductive filament and thus RESET process happens (Shi *et al.*, 2021). Figure 2.9 shows the TCM of Pt/Al/AIO_x/ITO device. During SET process in both unipolar and bipolar switching, the oxygen O²⁻ ions drift towards the top electrode due to Joule heating effect leaving oxygen vacancies accumulate at the AIO_x layer and set the device to LRS. The device switches to HRS when the conductive filaments break as it reaches the critical temperature when the positive bias voltage and current increases for the unipolar switching. Meanwhile for bipolar switching, the oxygen ions return back to AIO_x due to melting of the conductive filament when negative bias voltage is applied and the cell switches to HRS. In general, Joule thermal effect causes thermal decomposition thus enable the ions migration and switches the device from HRS to LRS while thermal melting reaction causes the rupture of conductive filaments and the cell returns back to HRS (Shen *et al.*, 2020).

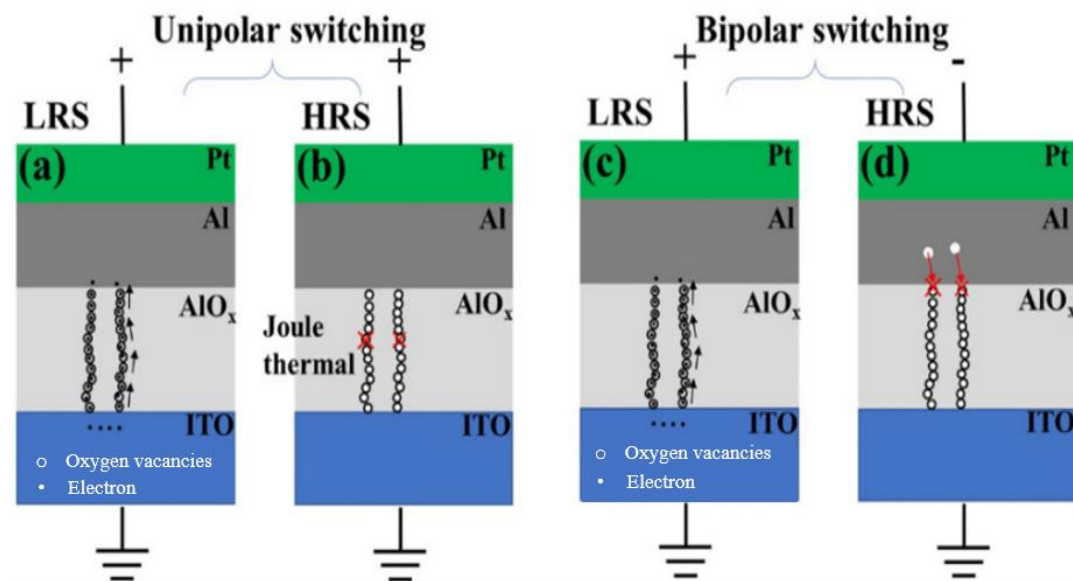


Figure 2.9 Thermochemical mechanism of AIO_x based resistive switching device with (a) (b) unipolar switching (c) (d) bipolar switching (Shen *et al.*, 2020).

2.4 Resistive Switching Materials

The materials in a resistive switching device includes the electrode material and switching material. Typically, the switching layer is an insulator or semiconductor. There are many forms of layer that have been investigated recently including nanoparticles, nanowires, two-dimensional (2D) materials, 3-D nanoarrays, etc (Wang *et al.*, 2020). The most common form is in thin film, which is our focus in this project. The resistive switching materials can be subdivided into inorganic, organic and bio-organic materials. Based on the perspective of Wang *et al.* (2020), inorganic materials have advancement in switching stability and manufacturing technology while organic materials better in mechanical flexibility and low cost. The inorganic and organic resistive switching thin film materials will be briefly discussed in this section.

2.4.1 Metal Sulfides Resistive Switching Materials

The earliest resistive switching inorganic thin film was metal sulfides or electrolytes with Cu or Ag elements (Shi *et al.*, 2021). Xu *et al.* reported the resistance switching characteristic of Ag/Ag₂S/W structure through high resolution transmission electron microscope (TEM) which shows the formation and rupture of ionic and electronic conductive path due to the Ag₂S argentite phase and Ag nanocrystal (Xu *et al.*, 2010). Fuji *et al.* (2011) also conducted similar experiment to real-time examine the conductive path in Cu-GeS electrolyte through TEM, selected area diffractometry (SAD) and energy-dispersive x-ray spectroscopy (EDX). It was found out that the conductive path was composed mainly Cu (Fujii *et al.*, 2011). The resistive switching in both Ag₂S and Cu-GeS electrolyte was mainly due to the electrochemical metallization mechanism (ECM). Although researchers showed the possibilities of sulphides materials to be used for resistive switching application with the resistive switching of metal sulphides devices having low working voltages as their ion migration

barrier are low (Xu *et al.*, 2010). However, they are incompatible with current CMOS process and thus restricting their practical applications (Shi *et al.*, 2021).

2.4.2 Perovskite Resistive Switching Materials

Meanwhile, perovskite was also widely investigated for resistive switching applications due to its defect chemistry (Shi *et al.*, 2021). There are two types of perovskite materials used which are perovskite oxide and perovskite halides. As such, Ignatiev *et al.* (2006) reported that the resistive switching mechanism in magnetite perovskite, $\text{Pr}_{0.7}\text{Ca}_{0.3}\text{MnO}_3$ (PCMO) thin oxide film was initiated at the interface region. It was an interface type valence change mechanism (VCM) where the current was driven by the oxygen ion/vacancy motion (Ignatiev *et al.*, 2006). Other than PCMO, Co-doped BaTiO_3 , Sr-doped LaMnO_3 , Nb-doped SrTiO_3 etc. has also been investigated as active layer in resistive switching device. Yin *et al.* (2014) showed a direct experiment evidence of Schottky barrier resistive switching mechanism of $\text{Ni/Nb:SrTiO}_3/\text{Ti}$ structure through an impedance spectroscopy. The relation between the charge trapping and de-trapping in the interfaces was due to the variation of Schottky barrier height. Other than that, perovskite halides such as $\text{CH}_3\text{NH}_3\text{PbI}_{3-x}\text{Cl}_x$ film also possess excellent resistive switching behaviour (Yoo *et al.*, 2015). Yoo *et al.* (2015) reported that the resistive switching was contributed by the construction of conductive filament from the migration and redistribution of defects in the perovskite film. It was proven that the resistive switching mechanism in perovskite can be metal-insulator transition, interfacial barrier modulation or conductive filament formation (Shi *et al.*, 2021).

2.4.3 Binary Metal Oxides Resistive Switching Materials

Other than perovskite, binary metal oxides also possess excellent resistive switching properties and have been widely discussed. As such, GeO_x -based RRAM

showed ultrahigh ON/OFF ratio of 10^9 (Rahaman *et al.*, 2012). Based on the reported article, the resistive switching mechanism in Cu/GeO_x/W device was due to formation and rupture of Cu nanofilament during the voltage sweep (Rahaman *et al.*, 2012). As reviewed by Kumar *et al.* (2017), most binary metal oxide possess resistive switching properties due to either metal ions migration, oxygen ions migration or pure electronic mechanism which the bulk film allows charge trapping and de-trapping or metal-insulator transition.

2.4.4 Organic Resistive Switching Materials

Other than inorganic based-ReRAM, organic materials that was used for resistive switching devices includes small-molecule materials or polymer-based materials (Shen *et al.*, 2020). The small molecule materials that had been explored were mostly semiconducting such as 2-amino-4,5-imidazoledicarbonitrile (AIDCN), tris-(8-hydroxyquinoline) aluminium (Alq₃), pentacene, etc (Gao *et al.*, 2019). The original structure consist of an Al/small molecule/metal nanoclusters/small molecule/Al system that was proposed by Ma *et al.* (2003). It was found that the resistive switching behaviour was due to the polarization in metal-nanocluster when sufficient voltage bias is applied (Ma *et al.*, 2003). Although small molecule organic materials show promising switching performances, but the deposition of metal-nanocluster is often hard to control, and the switching characteristic was not sensitive to the type of nanocluster or the semiconducting organic small molecule thus attention was given to organic small molecules that incorporate with donor-acceptor structure (Gao *et al.*, 2019). Figure 2.10 shows the device structure of organic memory device. As reviewed by Cho *et al.* (2011), there are four types of device structure in organic resistive switching devices that possess volatile or non-volatile switching. The structure includes I) single layer without nanoparticles, II) bilayer structure with two types of organic materials, III) trilayer

structure with nanoparticles placed in the middle of organic layer and IV) nanoparticles randomly blended with the organic materials (Cho *et al.*, 2011).

Although inorganic thin film were widely used in ReRAM due to their abundant resources, high stability, low-temperature processability and compatibility with the CMOS (Shi *et al.*, 2021) while organic thin film having advantages of low fabrication cost, printability and simple device structure (Cho *et al.*, 2011) but a more environmental friendly materials is needed in order to solve the electronic waste issue. Thus, our work focusses on resistive switching materials that are natural and biodegradable.

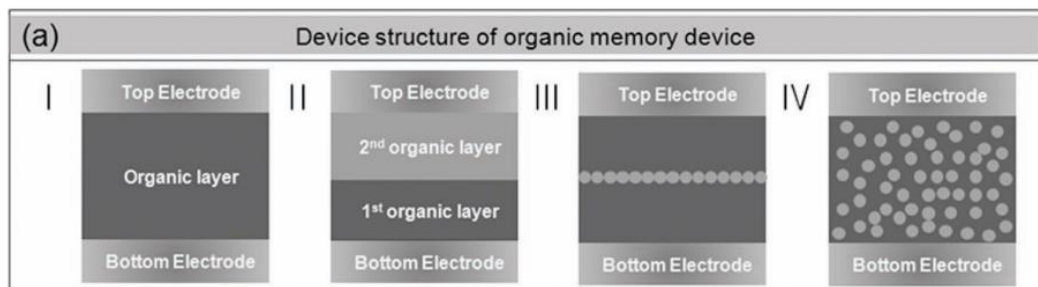


Figure 2.10 Various structure of organic resistive switching device (Cho *et al.*, 2011).

2.4.5 Bio-organic based Resistive Switching Materials

The use of bio-organic-based material for resistive switching memory application was first reported in 2006 by sandwiching tobacco mosaic virus (TMV) incorporated with platinum nanoparticles (Pt NPs) in a polyvinyl alcohol (PVA) matrix layer between two Al electrodes. The authors concluded that the resistive switching properties is attributed to charge trapping and de-trapping between the RNA and protein in TMV with the Pt NPs. The RNA serves as charge donors while protein stabilize the entrapped charges. This builds up the write and erase processes in the memory device (Tseng *et al.*, 2006). Subsequently, numerous scholars have conducted extensive research on processing bio-organic materials that originate from plants, viruses, living

or once-living things into thin film that exhibit resistive switching properties and can be categorized into four broad categories which are polysaccharide, polypeptide, virus, and plant extract (Cheong *et al.*, 2021).

2.4.6 Polysaccharides Materials

The reported natural materials that possess resistive switching properties in the broad categories of polysaccharides was listed in the Figure 2.11. The references were listed in Table 2.1. Polysaccharides are polymeric carbohydrates composed of long chains of monosaccharide units joined by glycosidic linkages with a general formula of $(C_6H_{10}O_5)_n$, $40 \leq n \leq 3000$ (Xu, 2017). Since honey contains mostly sugar which are glucose and fructose with chemical formula $C_6H_{12}O_6$, it was in the categories of polysaccharides.

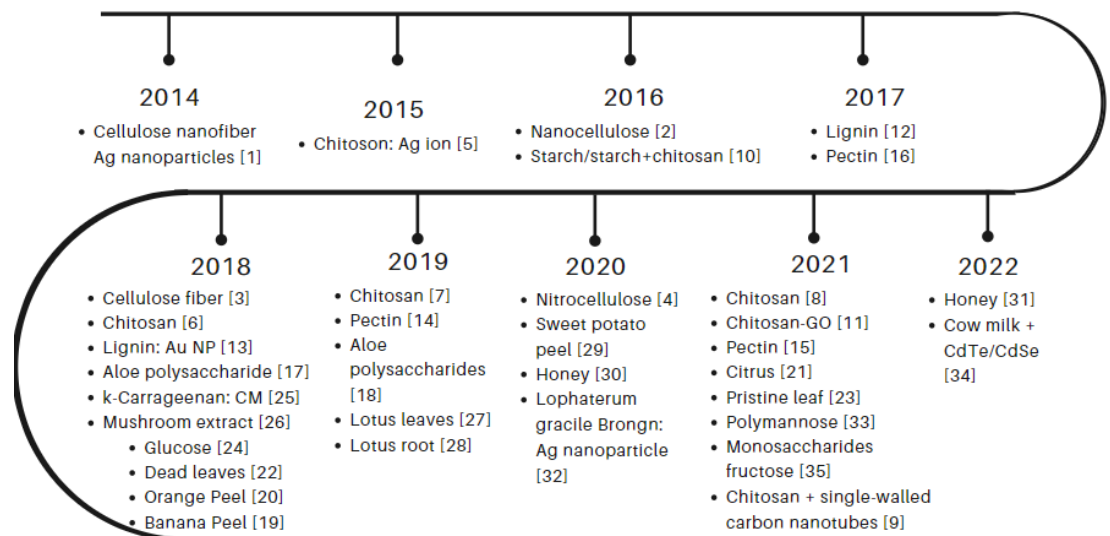


Figure 2.11: Bio-organic resistive switching materials based on polysaccharides.

The present of polysaccharides in the fabrication of thin film for resistive switching memory application was first found in 2014. The authors demonstrated the Ag-decorated cellulose nanofiber paper (CNP) sandwiched between Ag top electrode and Pt bottom electrode possess electrical switching behaviours through the small deviation of V_{set} and V_{reset} . The resistive switching mechanism was interpreted in terms

of formation and rupture of Ag conductive filaments (Nagashima *et al.*, 2014). Similarly, Ag-doped chitosan thin film also possess the same resistive switching mechanism, but the authors addressed that the HRS was controlled by space-charge-limited-conduction while the LRS was governed by ohmic and filamentary type of current conduction (Hosseini and Lee, 2015). These two papers critically evaluate the role of metal ions particle and electrode in governing the resistive switching mechanism. However, the role of polysaccharides natural materials chosen for their study was not technically discussed. The reason for choosing cellulose and chitosan is due to their flexibility and biocompatibility.

2.4.7 Glucose-based Resistive Switching Materials

In year 2008, Park *et al.* carried out experiment on the resistive switching behavior of glucose-based RRAM. In their research, they found out that the fabricated glucose-based RRAM shows a nonvolatile bipolar resistive switching behaviour with high endurance which possess stable switching to 100 consecutive cycles at low read voltage of 0.3V and data retention of 10^4 s (Park *et al.*, 2018). The reported switching mechanism of Al/glucose/p⁺ silicon was explained through the uniform formation of conducting filament through the observed uniform switching voltage distribution. The LRS of the device was governed by ohmic conduction behaviour as the fitting slope correspond to 1 while HRS was controlled by trap-controlled space charge limited current as the slope continuously increase from 1 to 3. Other than space-charge limited current, the authors also mentioned that there is formation and rupture of local conductive filament near the Al/glucose interface as the device exhibit abrupt current increase in transition of positive voltage sweep. Thus, the conducting filament was induced by the oxygen ion migration between Al/glucose layer as Al has high oxygen affinity and thus the oxide layer could form spontaneously with glucose layer as glucose

contain oxygen functional group. In order to verify the important role played by the oxidizing layer, Mo and Pt metal that have weak oxidizing tendency was also used to study the resistive switching behaviour of glucose-based RRAM. They observed both glucose-based RRAM with Mo and Pt top electrode possess poor resistive switching characteristics as there is no formation of oxidized interface metal layer when the electrode is replaced by a noble metal. Therefore, Park *et al.* conclude that the oxide layer plays an important role in resistive switching behaviour of glucose-based RRAM (Park *et al.*, 2018). Although the resistive switching properties of glucose-based RRAM has been investigated but their thermal effect against resistive switching behaviour was unknown. However, Park's research gives a guide on the possibilities of honey which contains glucose and fructose to be further explored for resistive switching applications.

2.4.8 Monosaccharide Fructose-based Resistive Switching Materials

Other than that, there was also reported monosaccharide fructose film that exhibit non-volatile resistive switching behaviour by Xing *et al.* The authors reported that the fructose RRAM exhibits better performances than glucose-based RRAM as it shows higher ON/OFF ratio and higher SET and RESET voltages. In the reported paper, fructose film with Ag and Al top electrodes were investigated and the mechanism was illustrated in Figure 2.12 below. At pristine state, oxide layer of Al was formed at the Al/fructose interface. Thus, at HRS in order to dissociate the oxide layer of Al, fructose film with Al top electrode requires higher V_{form} voltages. As shown in Figure 2.12 (f) and 2.12 (f'), the Al^0 and Ag^0 was oxidized into Al^+ and Ag^+ ions and drift towards bottom electrode through the defective sites respectively. After reaching the bottom electrode, the metallic ions were reduced to metallic elements and form a conductive filament up to the top electrode, changing the device from HRS to LRS. V_{set} for Al/fructose/ITO device was higher than Ag/fructose/ITO as the oxide formed in